# Uncertainty in Surface Microseismic Monitoring*

**Mike Mueller[1], Michael Thornton[1], and Leo Eisner[2]**

Search and Discovery Article #41258 (2013)
Posted December 23, 2013

*Adapted from extended abstract prepared in conjunction with poster presentation at AAPG International Conference and Exhibition, Cartagena, Colombia, September 8-11, 2013, AAPG©2013

[1]MicroSeismic Inc., Houston, TX (mmueller@microseismic.com)
[2]Institute of Rock Structure and Mechanics, ASCR, Prague, Czech Republic

## Abstract

Uncertainty in a migration based approach to surface and near surface microseismic monitoring occurs in two ways: uncertainty in the validity of detected events and uncertainty in the estimated position of the event. Synthetic modelling and comparison to case studies show that sign-to-noise-ratio is a key indicator of both types of the uncertainties. In this paper, we present an analysis of both types of uncertainty using synthetic modelling to illustrate the performance characteristics of the migration process in terms of signal detection and false-alarm rates, along with uncertainties in positional estimates.

Examples from two case studies will illustrate that this kind of performance is achievable in actual monitoring surveys. Signal-to-noise-ratio (SNR) is a key indicator of the uncertainty in migration-based imaging of microseismic events. Reliability, in terms of the ability to detect the complete set of events is a nearly binary function of SNR. Events with SNR above a threshold of 2-3 are readily detected, while events with SNR below the threshold are missed. Positional uncertainties likewise are driven by SNR. While vertical uncertainty is more sensitive to noise, both horizontal and vertical uncertainties decrease rapidly with increasing SNR.

## Introduction

Unconventional resource plays demand intense drilling and reservoir stimulation programs, and economic exploitation requires these resources be employed efficiently. Microseismic monitoring can provide important information to help optimize well placement and stimulation programs (Maxwell, 2010). Microseismic monitoring with surface arrays offers several advantages over borehole monitoring. Surface arrays do not require dedicated monitoring borehole, they offer a much larger field of view allowing long laterals to be monitored in their entirety and consistency (Duncan and Eisner, 2010). Moreover, surface deployment of large 2D or 3D arrays captures a large portion of the emitted microseismic wave field, enabling well-constrained event imaging with only compressional waves significantly reducing the sensitivity to velocity model assumptions. Furthermore, these arrays are well disposed for permanent monitoring of multiple wells.

The primary challenges in surface monitoring are: 1) increased distance between event hypocenter and receiver reduces signal size, 2) increased noise levels at surface. While borehole monitoring schemes typically rely on detection of events in the recorded traces followed by event location, the reduced signal-to-noise-ratio (SNR) at the surface does not generally allow detection of signals in the unstacked data (e.g., Zhebel et al., 2010). One approach to this problem is to apply a migration based imaging scheme to simultaneously improve the SNR and to position events at their proper location. In this approach, one must then rely on signal detection after migration, which leads to two levels of uncertainty: 1) uncertainty in the detection of signal, 2) uncertainty in the localization of the event.

In this paper, we present an analysis of both types of uncertainty using synthetic modeling to illustrate the performance characteristics of the migration process in terms of signal detection and false-alarm rates, along with uncertainties in positional estimates. Examples from two case studies will illustrate that this kind of performance is achievable in actual monitoring surveys.

## Imaging Method

Our migration-based approach to microseismic imaging involves three steps: downward continuation by beamforming, followed by event detection, then event localization (estimation of event location and timing). Beamforming is accomplished by a progressive scan of potential hypocenter locations in the subsurface. For each potential location, diffraction curves for compressional waves are computed, assuming a known velocity field. The recorded data traces are then summed across the array along the diffraction curves for the entire trace length. This beamformed trace forms a continuous estimate of the potential source at the subsurface location over the course of the recording.

As microseismic events are transient events, the next step is to identify and extract potential events from the continuous beamformed trace. Potential events are detected by an amplitude ratio test. The ratio of RMS amplitude within a sliding event window (the signal estimate) to the RMS amplitude in a trailing window (the noise estimate) is used to compute an estimated SNR. If the SNR exceeds a specified threshold, the event window is marked as a potential trigger.

Once all triggers are detected over all potential hypocenter locations, the catalog is analyzed to localize the event. Due to the finite extent of the array and the restriction of the array to the near surface, the point response of the migration will cause a single event to produce triggers spread across many subsurface locations. For a surface array with an aperture twice the depth of interest, this point spread function will be elongated in the vertical direction by roughly a factor of three compared to the horizontal response. This elongated shape is primarily an expression of the trade-off between time of the event (i.e., origin time) and depth of the event when origin time of the event is unknown (Eisner et al., 2009). The actual size of this response is determined by the frequency of the received signal, the velocity of the overburden, as well as the array configuration. The localization step consists of identification and evaluation of triggers related to a given event and a secondary diffraction sum along the time/depth trade-off trajectory (Duncan et. al., 2010). This secondary diffraction sum, allows us to estimate the timing and location of optimal energy focus and hence the event position.

## Uncertainty

Leaving aside uncertainty in the assumed velocity model, uncertainty arises in two primary contexts in this process. The first is in the detection step: How certain can we be that the detected events are, in fact, true microseismic events and not spurious noise? The second relates to the event localization: How accurate are the positional estimates, especially in the vertical direction?

Detection theory provides some insight into the first question (Johnson and Dudgeon, 1993). The basic test in detection theory is the choice between two hypotheses: $H_0$ = signal absent, and $H_1$ = signal present. The Neyman-Pearson lemma (1933) shows that it is possible to construct a likelihood ratio test to specify this choice, which minimizes the chances for incorrectly choosing $H_1$ when there is no signal present (a false alarm). The likelihood ratio test can be equivalently specified by a sufficient statistic, which is compared to some threshold value, where values of the statistic below the threshold indicate no signal present, and values above the threshold indicate the presence of signal. By specifying the test in this manner, one effectively fixes the probability of false alarms in the system. In general, it is not possible to choose a statistic/threshold combination that reduces the probability of false alarms to zero, so one must accept some probability of false alarms. In practice, one must balance the false alarm probability against the probability of failing to detect valid signal.

The SNR value we compute in the detection phase is such a sufficient statistic for a likelihood ratio test. The actual false-alarm probability in the system is determined by the distribution of noise after beam forming. If, for example, one were to assume the noise is Gaussian and the trailing window RMS measure is a valid estimate of the standard deviation of this distribution, then a SNR threshold value of two would result in a false-alarm probability of ~2.5% (the approximate cumulative probability of the Gaussian distribution above two standard deviations). Thus, for every 1,000 windows examined where there is in fact no signal, we should expect 25 false alarms with SNR greater than two. If we restrict ourselves to windows with SNR greater than three (false alarm probability of ~0.1%), we should expect to see only one false alarm. Therefore, under the assumptions listed above a SNR increase results in a decrease of the likelihood of a given trigger being a false alarm.

While it is difficult to assign a certainty to an individual detected event, detection theory does supply some useful insights to the event catalog as a whole. First, we know that the event catalog will contain some percentage of false alarms. Second, certainty in the event should increase with estimated SNR.

Estimating an event location ultimately comes down to selection of an optimal focusing point. Uncertainty in this estimate is driven by the effect of noise in this selection process. While the particulars of how noise interacts with the selection process are specific to the selection algorithm, we can predict that noise will tend to move the estimated location along contours of the migration point response and that the impact of noise should decrease with increasing SNR.

## Synthetic Modeling

In order to assess both types of uncertainty, we constructed a synthetic data set that was used in our imaging algorithm to locate events with varying amounts of noise. The synthetic data set consisted of a surface array of 1,000 channels arranged in a radial pattern of eight arms equally spaced in azimuth. Each arm consists of 125 channels spaced at 100 feet with an initial offset of 1,000 feet from the center of the array resulting

in a maximum offset of 13,400 feet. 100 events at a depth of 10,000 feet and located near the center of the array were modeled using a 30 Hz center frequency minimum-phase Ricker wavelet with a constant moveout velocity of 12,000 feet/s.

For a range of input SNR levels (0.02-20), Gaussian noise was added to the modeled data and imaged with the migration routine with the detection threshold set at two. The event catalog output by the migration was then compared to the known origin times and locations of the modeled events. A detected event with an origin time within 100ms of a modeled event was considered a true detected event (a hit) while all other events are considered false alarms.

Figure 1 shows number of hits and false alarms for each output SNR level. For SNR > 2, all 100 of the seeded events were detected. For SNR < 2, the detection rate rapidly drops, effectively reaching zero for SNR < 1. This behavior suggests that we can use SNR as an indicator of reliability in the performance in the algorithm. Above some SNR threshold, valid events are reliably detected, while below this threshold valid events are missed.

For all output SNR levels, the number of false alarms remains approximately constant at a value of 10. While constancy is expected from detection theory, this value is much lower than one might expect for a 2.5% false-alarm rate. The 100 events were seeded at 2-second intervals into a 200-second long data set sampled at 4ms. In the triggering routine, the event window moves forward sample by sample. Thus, we examine 50,000 potential triggers and should expect 1,250 false alarms in the triggering phase. However, the ten false alarms shown in Figure 1 are those that were triggered but also passed the event localization step. Part of the event localization step is a requirement that the triggers show consistency over the time/depth trade-off trajectory. If the algorithm fails to find this consistency, the trigger is discarded. Thus, we add further constraint against false alarms.

Figure 2 shows the standard deviations of positional errors computed from the matched events (hits) shown above. Not shown in the figure are the average errors, for SNR > 1 average errors are very close to zero for all three dimensions indicating the estimates are unbiased. For SNR > 1, we see an exponential decline in variability of the errors, with horizontal and vertical uncertainties converging to near zero for very high SNR values. Variability in X and Y are approximately equal and 2-3 times smaller than variability in Z. The rate of decline in variability in all three dimensions is approximately the same. The estimates with SNR < 1 should be discounted as it contains only two hits, and origin time errors associated with these two hits are significantly larger than the other hits (50ms vs. 5ms), indicating these are not likely valid matches.

As predicted, sensitivity to noise in the vertical direction is greater than in the lateral direction. The relative magnitude of the vertical and horizontal sensitivity is roughly proportional to the elongation of the migration point spread response. Furthermore, the impact of noise on the positional estimates diminishes rapidly with increasing SNR.

## Case Studies

Table 1 summarizes the analysis of uncertainty in two calibration studies from separate hydraulic fracture monitoring surveys in two different shale plays in North America. Both utilized radial surface arrays similar to the one used in the synthetic modeling. Approximately 1,000 channels were used in each; the channel spacing was varied to maintain an aperture twice the depth of interest. In both cases, perforation shots

were used to calibrate the velocity and static corrections for the array. Once the calibration was determined, the imaged positions of the detected perforation shots were compared to the measured location of the gun. The SNR range for the set of shots and the standard deviation of the errors are reported. The estimated uncertainties in positions may be subject to a systematic bias as measured locations of perforation shots can be offset due to errors in deviation surveys (see Bulant et al.
2007).

In Case #1, 85 shots were imaged over a pad of five lateral wells. Even though all the shots used similar charges, the SNR range varied from 3 to 10, with 60% of the shots having a SNR < 5. The difference SNR is likely result of variable conversion of charge energy to seismic energy as also observed by Chambers et al. (2010). We consider SNR < 5 to be low SNR for calibration. Average errors in all three dimensions were less than 30 feet.

In Case #2, 28 shots were imaged over a single lateral well. Although the target here was much deeper than the first case, the SNR range is considerably higher, with 78% of the shots having a SNR >15. We consider this to be very good SNR for calibration. Average errors in all three dimensions were less than 20 feet.

While the positional uncertainties in both cases are larger than those shown in the synthetic model, they do show a similar behavior. Case #2, which is characterized by a larger SNR, shows a smaller uncertainty indicated by a smaller standard deviation of the errors. Case #2 also shows similar uncertainties in horizontal and vertical directions comparable to the convergence noted in the synthetic model. We believe the increased uncertainty compared to the model is due to the need to estimate velocity and static corrections and the presence of coherent noise in real data. In both cases, the uncertainties reported here were deemed acceptable by the operator.

## Conclusions

Signal-to-noise-ratio (SNR) is a key indicator of the uncertainty in migration-based imaging of microseismic events. Reliability, in terms of the ability to detect the complete set of events is a nearly binary function of SNR. Events with SNR above a threshold of 2-3 are readily detected, while events with SNR below the threshold are missed. Positional uncertainties likewise are driven by SNR. While vertical uncertainty is more sensitive to noise, both horizontal and vertical uncertainties decrease rapidly with increasing SNR.

While SNR can be used to infer the relative likelihood that given event is real, false alarms will occur. Discriminating the real event from the false will require additional information beyond SNR.

While synthetic modeling is useful in assessing the performance characteristic of the imaging method, a number of simplifying assumptions were made that differ from actual application of the method. First, our model assumed that travel-times were known exactly. In practice, velocity and static corrections must be estimated from calibration shots (sources at known locations in the subsurface). While travel time errors are most likely to decrease the SNR after migration, long period errors in travel times could cause spurious focusing and add uncertainty.

Secondly, the model assumed the additive noise was Gaussian. While this is a reasonable first approximation, it does not take into account coherent noises, which are ubiquitous in surface microseismic monitoring. Appropriate preprocessing can reduce the impact of coherent noise, but residual coherent noise will trigger false-alarms. Moreover, the number of false alarms rejected in the event localization step will likely not be so high, as coherency in the noise will imply some additional consistency among triggers not seen in the model.

## References Cited


Bulant, P., L. Eisner, I. Psencik, and J.L. Calvez, 2007, Importance of borehole deviation surveys for monitoring of hydraulic fracturing treatments: Geophysical Prospecting, 55, no. 6, p. 891–899.

Chambers, K., S. Brandsberg-Dahl, J.-M. Kendall, and J. Rueda, 2008, Testing the ability of surface arrays to locate microseismicity: 78th Annual International Meeting, SEG, Expanded Abstracts, p. 1436–1440.

Duncan P. and L. Eisner, 2010: Reservoir characterization using surface microseismic monitoring: Geophysics, 75, p. 75A139–75A146.

Duncan, P.M., J.D. Lakings, and R.A. Flores, 2010, Method for passive seismic emission tomography: U. S. Patent 7,663,970 B2.

Eisner, L., P.M. Duncan, M. Heigl, and W.R. Keller, 2009, Uncertainties in passive seismic monitoring: The Leading Edge, v. 28, p. 648–655.

Johnson, D.H. and D.E. Dudgeon, 1993, Array signal processing: concepts and techniques: Prentice Hall, Englewood Cliffs, New Jersey, 533 p.

Maxwell, S., 2010, Microseismic: Growth born from success: The Leading Edge, v. 29, p. 338–343.

Neyman, J. and E. Pearson, 1933, On the problem of the most efficient tests of statistical hypotheses: Philosophical Transactions of the Royal Society of London, v. 231/694–706, p. 289–337.

Zhebel, O., D. Gajewski, and C. Venelle, 2010, 80th Annual International Meeting, SEG Expanded Abstracts, v. 29, p. 2181–218.

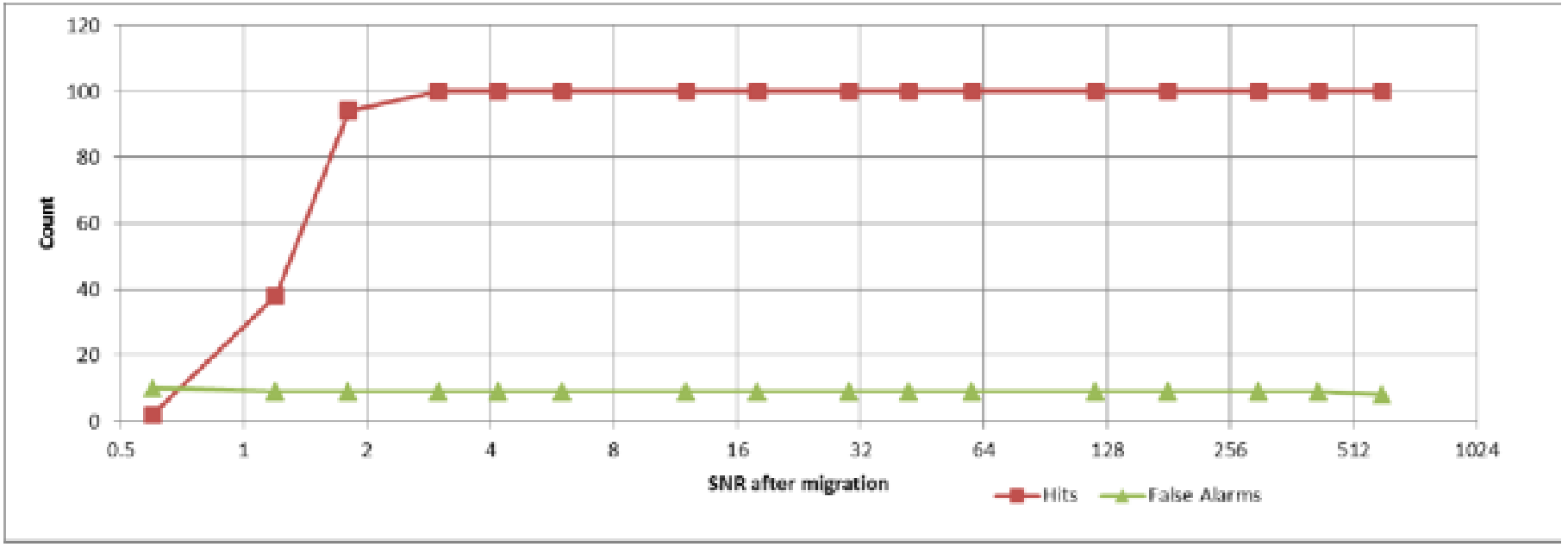


Figure 1. Count of detected events as a function of SNR after migration. Detected events matched to modeled events are shown as hits; events without a match are shown as false alarms.

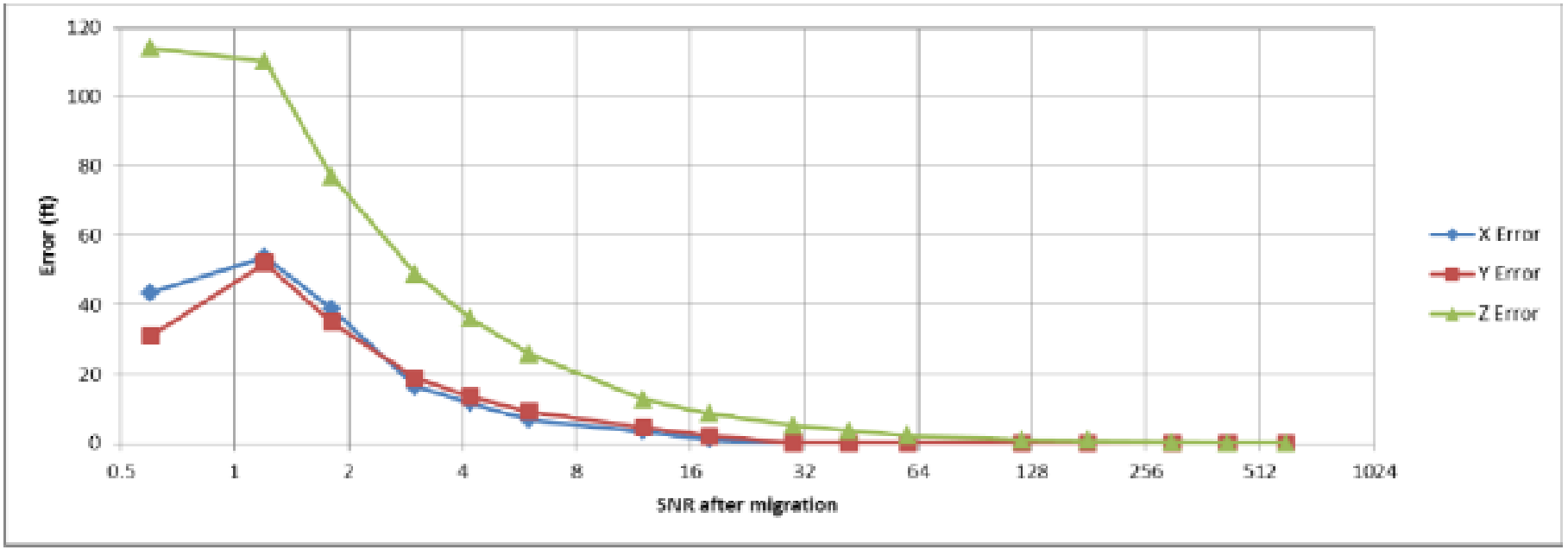


Figure 2. Standard deviation of positional errors as a function of SNR after migration.

| Case Study | Number of events | Depth Of Target (ft) | SNR Range | Std. Dev. X error (ft) | Std. Dev. Y error (ft) | Std. Dev. Z error (ft) |
|---|---|---|---|---|---|---|
| 1 | 85 | 7,000 | 3-10 | 76 | 106 | 116 |
| 2 | 28 | 11,000 | 8-30 | 51 | 59 | 52 |

Table 1. Summary of uncertainty in calibration errors in two case studies.